Materials Science and Engineering C 29 (2009) 172–177

Contents lists available at ScienceDirect

Materials Science and Engineering C

journal homepage: www.elsevier.com/locate/msec

Preparation and characterization of dense nanohydroxyapatite/PLLA composites

Sandrine Gay *, Saioa Arostegui, Jacques Lemaitre

Laboratory for Powder Technology, EPFL, MX-Ecublens, CH-1015-Lausanne, Switzerland

ARTICLE INFO

Article history:
Received 10 March 2008
Received in revised form 21 May 2008
Accepted 10 June 2008
Available online 17 June 2008

Keywords:
PLLA
Nano-hydroxyapatite
Dense composite
Bone substitute
Mechanical properties

ABSTRACT

Synthetic bone graft substitutes based on PLLA have been largely studied during the past decade. PLLA/hydroxyapatite composites appear as promising materials for large bone defect healing. In this study dense PLLA/nano-hydroxyapatite composites were prepared by hot pressing. Dense samples were investigated rather than porous scaffolds, in order to shed light on possible correlations between intrinsic mechanical properties and nano-hydroxyapatite concentration. Hydroxyapatite deagglomerated by wet attrition milling, and further dispersed into chloroform was used (median diameter=80 nm). Particle size distribution measurements and transmission electron microscopy show evidence that particle size and dispersion are maintained throughout the successive steps of composite processing. Mechanical properties were tested (uni-axial and diametral compression tests) as a function of nano-hydroxyapatite content. Increasing concentrations of nano-hydroxyapatite (0, 25 and 50 wt.%) increase the Young's modulus and the mechanical strength of the composite; at the same time, the failure mechanism of the material changes from plastic to brittle. Young's modulus over 6 GPa and uniaxial compressive strength over 100 MPa have been achieved. These values expressed in terms of intrinsic tensile and shear strengths indicate that 50 wt.% nano-hydroxyapatite containing samples develop properties comparable to those of cortical bone. PLLA/nano-hydroxyapatite composites are thus promising candidates to develop bioresorbable porous bone substitutes showing superior mechanical performance.

1. Introduction

Synthetic bone graft substitutes play an increasing role in large bone defect healing. A major challenge in the development of adequate bone substitutes is to obtain good initial mechanical stability together with fast osteointegration and resorption after implantation; this means that the implant material should develop superior intrinsic mechanical properties, and at the same time show optimal interconnected porous architecture.

A careful literature survey has shown that polymer/calcium phosphate composites are complex systems [1]. Material science teaches that final implant properties depend on numerous parameters: the most obvious are polymer characteristics (chemical composition, molecular weight, crystallinity [2,3]), and calcium phosphate characteristics (chemical and mineralogical composition, particle size distribution, aspect ratio, spatial distribution, particle/polymer interaction, concentration…) [4–9]. Moreover, preparation conditions have a crucial effect on the final properties of the material [10]. The most popular bioresorbable composite bone substitutes are based on hydroxyapatite/poly-L-lactic acid mixtures (HA/PLLA), since the raw materials are already approved for human clinical use and their degradation products are easily metabolized. Other polyesters can be used, such as polylactic–polyglycolic block copolymers (PLGA), or polycaprolactone (PCL) [11,12]. Degradation time can be tailored by playing on the ratio of the constitutive polymers. Hydroxyapatite is used for its well known biocompatibility, its crystallographic structure close to that of bone mineral, and its osteoconductive character. Other calcium phosphates such as β-tricalcium phosphate (β-TCP), amorphous calcium phosphate (ACP), biphasic calcium phosphate (BCP) are also proposed [12,13]. The main expected advantage of using ceramic particles such as calcium phosphates is to enhance the mechanical properties and provide calcium and phosphate delivery during implant resorption. The particle size distribution of the ceramic fraction is mostly in the micron range, but recent studies focus more and more on nanosized particles [5,8]. By this way, physical features closer to natural bone can be obtained [14–16].

From the tissue engineering viewpoint, pore size distribution, pore interconnectivity, surface chemistry, calcium availability [7], and incorporation of drugs or proteins are expected to influence migration, proliferation and differentiation of bone cells into a composite scaffold.

Three factors are expected to affect the final macroscopic properties of a composite material: polymer crystallinity, ceramic content and porous structure. Dense samples can be made by forging [17], by hot or cold pressing. Controlling processing factors such as pressure, temperature and cooling rate is essential [8]. Introduction of porosity

* Corresponding author. EPFL/IMX/LTP, Station 12, CH-1015 Lausanne, Switzerland. Tel.: +41 21 693 68 87; fax: +41 21 693 30 89.
E-mail address: sandrine.gay@epfl.ch (S. Gay).

0928-4931/$ – see front matter © 2008 Elsevier B.V. All rights reserved.
doi:10.1016/j.msec.2008.06.005

Table 1
HA particle size distributions

	Method	D_{v50}
HA raw powder	XDC[a]	2.1 μm
nHA in aqueous suspension	XDC	80 nm
nHA in chloroform	CPS[b]	<100 nm

[a] X-ray Disc Centrifuge (XDC, Brookhaven BI-XDCP).
[b] Centrifugal Particle Size analysis (CPS, CPS Instruments Inc).

is usually achieved by various processes such as solvent casting/particle leaching [18], phase separation [19,20], foaming [21], and fast prototyping [22].

In order to isolate the effect of nano-hydroxyapatite particles incorporation on the bulk properties of HA/PLLA composites, this study is focused on dense materials, in a hope to gain clear information on their intrinsic mechanical properties.

2. Materials and methods

2.1. Hydroxyapatite

HA powder (S_{BET}=68 m^2/g, D_{V50}=2.1 μm) supplied by Riedel de Haen (Switzerland, Ph. Eur) was deagglomerated in the laboratory, using attrition milling in aqueous solution (0.1 wt.% poly(acrylic acid) (PAA), neutralized with ammonia: R=[NH_3/Carboxyl]=1.5).

After deagglomeration, nHA was transferred into chloroform by using an ultracentrifugation separation technique: particle and solvent were separated by ultra-speed centrifugation (15,000 rpm, 20 min, Jouan GR 2022); after discarding the supernatant, the centrifugate was redispersed by ultra-sonication in a new solvent aliquot (US horn, Telsonic DG, 10 W, 15 min). As chloroform is not miscible with water, a first solvent exchange was performed from water to ethanol, followed by a second one from ethanol to chloroform.

Particle size distribution was checked after completion of the solvent exchange step. The size distribution of nHA remains unaffected by solvent exchange, as shown in Table 1. The final nHA concentration was measured gravimetrically after full solvent evaporation.

2.2. Poly-L-lactic acid

Poly-L-lactic acid (PLLA) was purchased from Lactel Absorbable Polymer (USA, #A06-072). The inherent viscosity is 1.04 dL/g. Molecular weight was measured by gel permeation chromatography. Polymer properties are summarized in Table 2. PLLA was dissolved into chloroform in order to facilitate sample preparation (7 wt.%).

2.3. Samples preparation

Three nHA concentrations were tested (0, 25, 50 wt%). Prescribed quantities of nHA suspension according to sample volumes and suspension concentration were weighed and mixed with polymer solutions. Table 3 summarizes the amounts of raw materials needed to prepare individual test specimens. Solutions were kept under magnetic stirring for 2 h at room temperature.

Table 3
Composition of the samples made for mechanical testing

	h [mm]	Ø [mm]	V [cm^3]	PLLA [g]	nHA [g]
Uni-axial compression	15.0	10.0	1.18		
Pure PLLA				1.460	0.0
PLLA+25 wt.% nHA				1.291	0.430
PLLA+50 wt.% nHA				1.048	1.048
Diametral compression	6.8	10.0	0.53		
Pure PLLA				0.662	0.0
PLLA+25 wt.% nHA				0.585	0.195
PLLA+50 wt.% nHA				0.475	0.475

In order to improve the uniformity of mixing, PLLA-nHA-chloroform mixtures were transferred into a syringe and extruded through a Kenics linear mixer (8 elements, Ø=5 mm). In this way the characteristic distance of heterogeneity was decreased down to less than 20 μm (5000 μm/2^8). The solutions were cast into Petri dishes (Ø=14 cm). The dishes were left under a fume hood at room temperature for 40 h, in order to allow full evaporation of chloroform.

Polymer and composite films were cut into small bits a few millimetres in size. Prescribed quantities of composites were weighed, and loaded into cylindrical stainless steel moulds (Ø=10 mm), preheated for 30 min at 190 °C. The samples were kept in their moulds for 20 min with the stainless steel piston in place. The moulds were then transferred to a manual hydraulic press, and kept for 2 min under a pressure of 300 MPa. The pressing temperature was estimated to be approximately 160 °C. After pressing, the samples were left for 5 min in the mould before being pulled out. After preparation, they were stored at room temperature under dry atmosphere before use.

Half of the total number of samples was annealed according to the experimental design (2×3, n=3) presented in Table 4. The specimens were kept in a preheated oven at 115 °C for 1 h, and then cooled down to room temperature in dry atmosphere [5]. The annealing step was performed at about 10 °C above the crystallisation temperature, in a hope to enhance the crystallinity of the polymer.

2.4. Samples characterizations

2.4.1. Relative density

The relative density of samples was calculated as the ratio of geometrical density and the density measured with a helium pycnometre (Micromeritics, Accu Pyc 1330). The geometrical density was estimated from the dimensions and weights of the cylindrical specimens.

2.4.2. Wetting angle

Wetting angles were measured on the unpolished basal surface of the specimens with a 5 μL water droplet. (Data physics Instruments GmbH). The wetting angle was fitted with the Young–Laplace's equation. Measurements were made in triplicate on each specimen.

Table 2
Properties of raw PLLA

	PLLA
Nature	Semicrystalline
Mw	104,000 g/mol
Tg	57 °C
Tm	176 °C
Viscosity index	1.04 dL/g

Table 4
Multifactorial experimental design 2×3, n=3

Factor	Definition	Levels		
		−1	0	1
A	Annealing	No	–	Yes
B	HA concentration [wt.%]	0	25	50
C	Replicate	I	II	III

2.4.3. Mechanical tests

Two mechanical testing modes were used: uni-axial compression and diametral compression.

Mechanical tests were performed on UTS machine (UTS Testsystem) using a load cell of 100 kN and a rate of 1.0 mm/min until failure. Displacement was measured with a LVDT displacement probe (Linear Variable Differential Transformer). Stress–strain curves were plotted.

Compressive Young's moduli were estimated from the slopes of the initial linear region of the stress–strain curves. Uniaxial or diametral compressive stresses on failure were taken as the stress values corresponding to a 2% difference between the expected elastic strain (ε) and observed strain (ε_x). They are called in this study compressive yield stress (σ_c) and diametral compressive yield stress (σ_b), respectively. In this way, it is possible to compare different types of failure behaviours.

$$\frac{\varepsilon_x - \langle\varepsilon\rangle}{\langle\varepsilon\rangle} \geq 2\%$$

From σ_c and σ_b, the Mohr's circles theory allows a plane representation of the three-dimensional state of stress acting on any given point of a mechanically loaded structure (Fig. 1); thus, it is possible to estimate the intrinsic material properties, expressed in terms of intrinsic tensile and shear strengths [23]. These intrinsic mechanical properties can be compared to those of bone.

2.4.4. Thermal properties

The thermal characteristics of PLLA and nHA/PLLA composites were measured by Differential Scanning Calorimetry (DSC, Q100 TA Instrument). Two temperature cycles were applied: a first run from 25 to 200 °C (15 °C/min), allowing to see the effect of composite processing, was followed by a fast cooling step (−15 °C/min) intended to quench the polymer in its vitreous state; then, a second run from 25 °C to 200 °C allows to see the effect of composition on the crystallisation and melting temperatures.

The crystallisation degree χ_c is calculated as the ratio of the observed melting enthalpy during the first run ΔH_{mPLLA} (J/g) to the theoretical value (203 J/g) [18]; no peaks of recrystallisation were found.

$$\chi_c = \frac{\Delta H_{mPLLA}}{203}$$

2.4.5. Microscopy

Microtome layers (thickness around 40 nm) were observed under Transmission Electron Microscopy (TEM, Philips CM20 Instrument). Particle size and spatial distribution of nHA particles throughout the polymer matrix were examined.

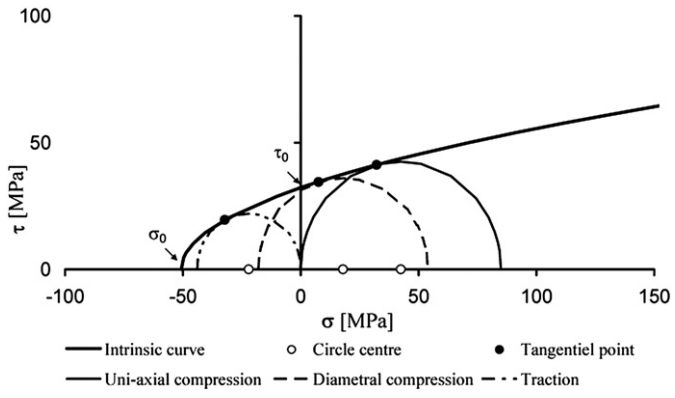

Fig. 1. Mohr's circle diagram.

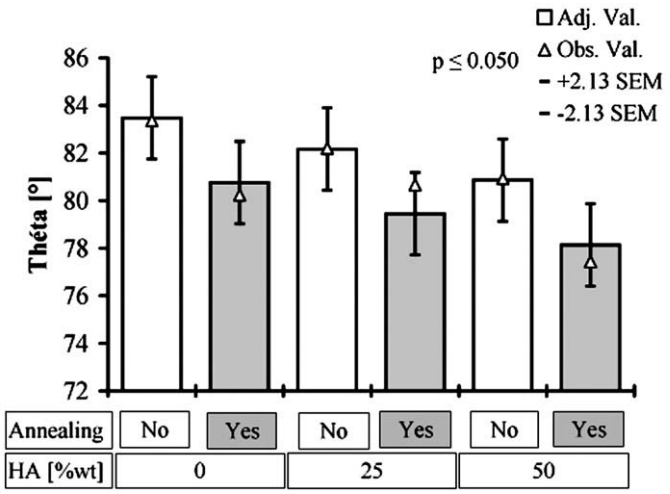

Fig. 2. Contact angles, as a function of annealing treatment and nHA content.

2.4.6. Thermogravimetric analysis (TGA)

The actual nHA concentration was measured by a thermogravimetric analysis under air, from room temperature up to 900 °C with a temperature rate of 10 °C/min (TGA/SDTA 851 Mettler Toledo). About 10–20 mg of composite were used.

2.4.7. Statistics

Statistical analysis of the results was performed by ANOVA. By default, the accepted type I error risk (α) was taken as 5%.

3. Results

3.1. Density

In all cases, densities higher than 97% of the theoretical density were achieved. No significant effect of HA content on density was observed.

3.2. Wetting angle

Annealing treatment and addition of nHA have a significant effect on wettability. Annealing appears to have the most significant effect (Fig. 2). The presence of nHA decreases the wetting angle slightly and thus improves wettability. This can be explained by the fact that HA

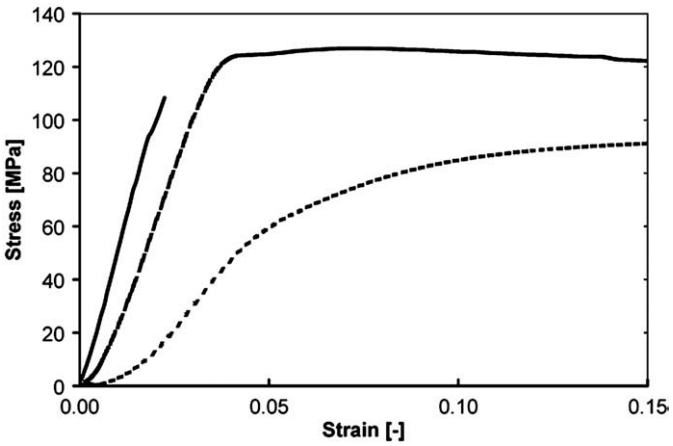

Fig. 3. Typical stress–strain curves in compression, as a function of nHA content. Dotted line: control PLLA without HA; Dashed line: PLLA+25 wt.% HA; Full line: PLLA+50 wt.% HA.

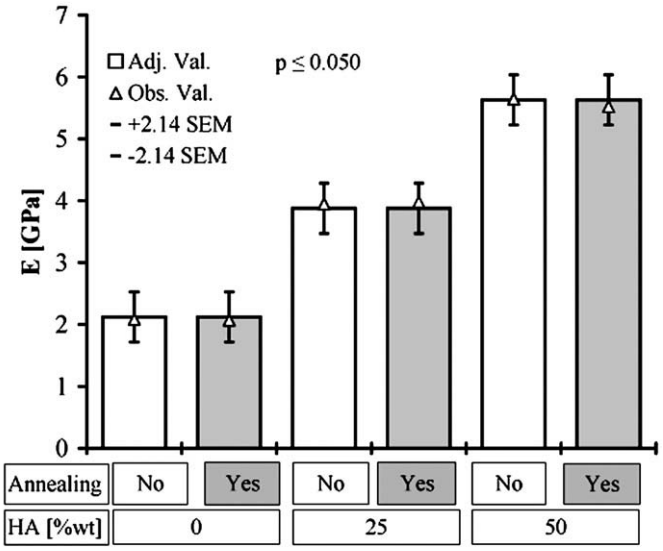

Fig. 4. Young's modulus as a function of annealing treatment and nHA content.

particles are more hydrophilic than PLLA. The annealing treatment also decreases the wetting angle. Several explanations can be proposed: 1) residual chloroform might remain at the surface of the specimens, which is more thoroughly eliminated after a 1 h annealing treatment, hence decreasing its hydrophobic contribution; 2) chemical surface modifications (oxidation or hydrolysis) might occurs upon annealing in ambient atmosphere. Further surface characterization, such as XPS (X-ray-Photoelectron Spectroscopy) would help to clarify this point.

3.3. TGA

Thermogravimetric results point to observed weight concentrations lower than the expected ones: 22.5% and 45.8% instead of 25% and 50%, respectively. The difference comes from overestimated nHA concentrations in chloroform suspensions, in which the contribution of residual PAA was not taken into account: indeed, some residual PAA remains adsorbed on nHA particles after completion of the solvent

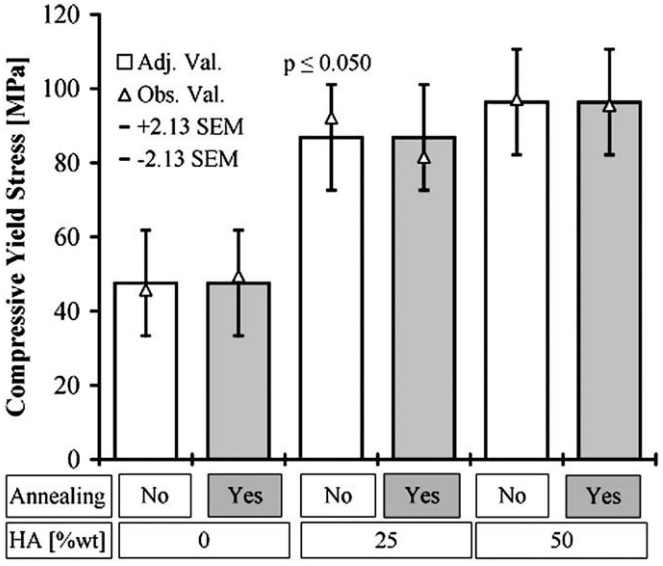

Fig. 5. Compressive yield stress as a function of annealing treatment and nHA content.

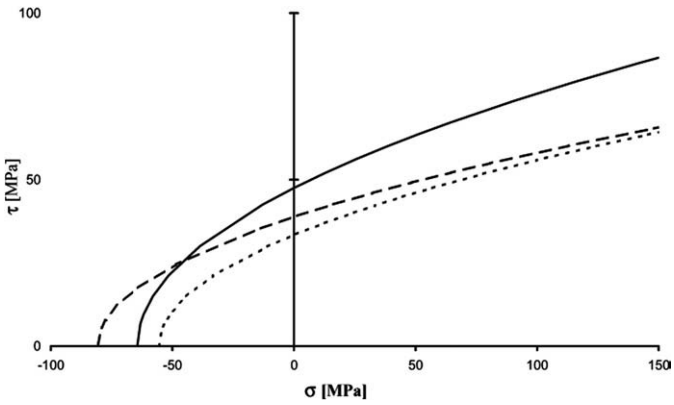

Fig. 6. Comparison of intrinsic characteristic curves of nHA-PLLA composites. Dotted line: PLLA+25% wt HA; Dashed line: PLLA+50 wt.% HA; Full line: Cortical bone, calculated from σ_{cmin}=130 MPa, σ_{tmin}=60 MPa (Ref [24]). Pure PLLA behaviour does not fit to this model.

exchange process. Nevertheless, for the sake of simplicity, nominal concentrations will be used throughout the text.

3.4. Mechanical testing

The concentration of dispersed mineral particles has a significant effect on the rupture mode, as shown in Fig. 3: without nHA, plastic

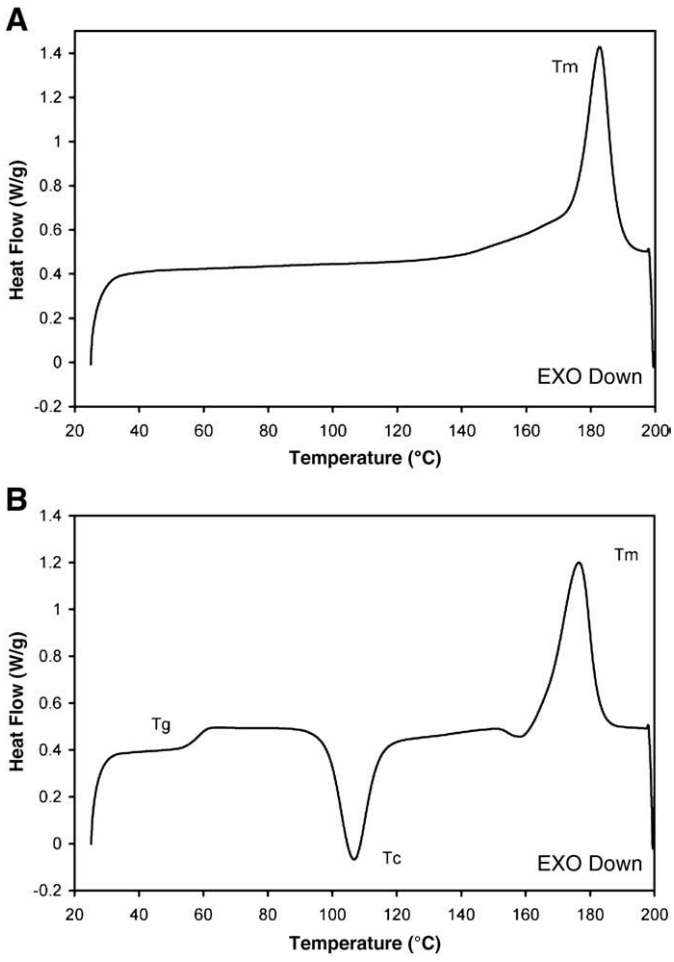

Fig. 7. Typical DSC curves of nHA-PLLA composite. A) First heating run; B) Second heating run.

deformation of the specimens occurs, resulting in a barrel shape without rupture; with 50 wt.% nHA, specimens show a typical brittle fracture, right away after an initial elastic deformation; with 25 wt.% nHA, an intermediate failure behaviour is observed: in that case, samples do not form a barrel, but no brittle fracture occurs.

The Young's modulus of PLLA without nHA particles is around 2 GPa. It increases in the presence of nHA particles. With 50 wt.% nHA, the elastic modulus is close to 6 GPa as represented in Fig. 4. In this range the change is linear with respect to nHA concentration. The Young's modulus is not significantly affected by annealing.

Fig. 5 shows the evolution of the compressive yield stress σ_c as a function of nHA concentration: no significant effect of annealing is observed. For samples containing 50 wt.% nHA, a σ_c of 96 MPa is obtained.

By drawing the intrinsic characteristic curves of the nHA/PLLA composites (Fig. 6), it can be seen that the concentration of nHA improves the cohesion of the material estimated by σ_0. Intrinsic tensile and shear strengths get closer to those of cortical bone. Pure PLLA is not represented here because its failure behaviour does not fit to the Mohr's model.

3.5. Thermal properties

Fig. 7 shows a typical behaviour of composite. Specific values according to the different treatments are given in Table 5.

In the first heating run of thermal analysis, only peaks related to the melting point are observed as shown in Fig. 7 (A); no significant effects are observed due either to nHA content or to annealing treatment. With the applied preparation protocol, the polymer has reached its ultimate crystallinity at the end of the cooling step, so that annealing does not affect the crystallinity of the material (χ_c env. 25%). The cooling rate during the preparation seems to be slow enough as to allow extensive crystallization. This also helps to understand why annealing does not affect significantly the mechanical properties.

In the second heating run, for which the history of sample preparation is erased, glass transition, crystallisation and melting points are observed as shown in Fig. 7 (B). Glass transition increases slightly with HA content but no significant changes in crystallisation and melting temperatures due to composition or annealing can be observed.

3.6. Microscopy

Fig. 8 shows transmission electron micrographs, corresponding to 50 wt.% nHA/PLLA composite samples, giving a feeling of the distribution of nHA particles throughout the PLLA matrix. Picture B with higher magnification confirms that the size of nHA particles is lower than 100 nm. The state of dispersion of the nHA particles achieved in the attrited aqueous suspension is clearly preserved in the final composite material. An even more uniform spatial distribution would probably be achieved by adding extra elements to the Kenics mixer. More uniform distribution of nHA particles throughout the composite matrix would improve further the final mechanical properties.

Table 5
Characteristic DSC temperatures of PLLA and PLLA/nHA composites according to nHA content and annealing treatment

	First heating run			Second heating run		
	T_m [°C]	ΔH_m [J/g]	X_c [%]	T_g [°C]	T_c [°C]	T_m [°C]
Pure PLLA	180.04	51.09	25.11	55.34	109.31	174.01
Pure PLLA annealed	182.48	54.32	26.71	56.99	109.16	174.82
PLLA+25 wt.% nHA	179.10	46.73	22.9	57.18	108.07	176.42
PLLA+25 wt.% nHA annealed	182.69	55.25	27.16	58.48	106.71	176.51
PLLA+50 wt.% nHA	179.02	49.33	24.25	62.22	107.81	177.67
PLLA+50 wt.% nHA annealed	179.11	48.32	23.80	61.42	106.35	176.05

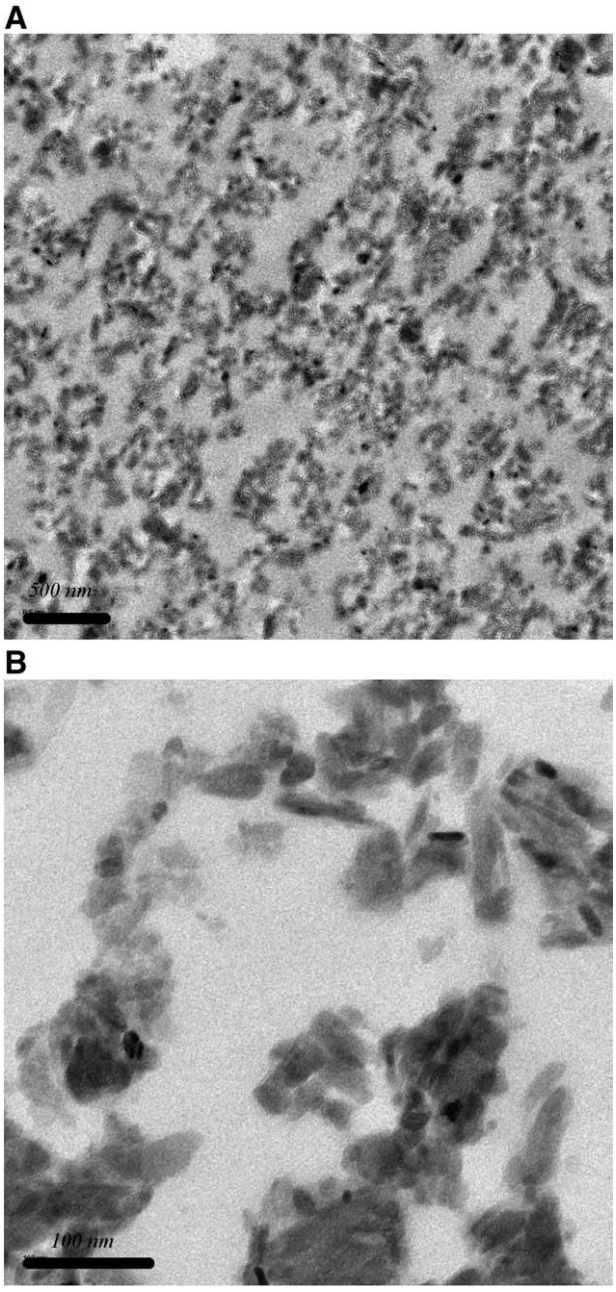

Fig. 8. TEM micrographs of nHA-PLLA composite (50 wt.% nHA, at two different magnifications (A: 5000×, B: 38,000×).

4. Discussion

Solvent casting/hot pressing technique allowed to prepare nHA/PLLA dense composites with high relative density and mineral content up to 46 wt.%, whose mechanical properties are comparable to bone.

The processing route developed in the present work allows to keep unaffected the HA particles dispersion throughout the processing steps, from initial attrition milling to final composite, as observed by TEM analysis.

Table 6
Literature examples of dense composites PLLA/hydroxyapatite mechanical properties

	Tested materials				Mechanical properties					
	Initial PLLA molecular weight [kDa]	Filler characteristics	Process conditions	Annealing treatment	Tension [MPa]		Compression [MPa]		Bending [MPa]	
					Failure strength	Elastic modulus	Failure strength	Elastic modulus	Failure strength	Elastic modulus
Okuno et al. 1999 [17]	220	None	103 °C, -, -	No	154.10	1300	123.5	4800	258.5	6500
	202	HA, 50 wt.%, 0.3–20 μm			103	2400	115	6500	267.5	12,300
Abe et al. 2001 [9]	160	None	180 °C, 40 MPa, 15 min	No					52	3500
		HA fibers, 70 wt.%, 40–150×2–10 μm							40	11,000
Uskokovic *et al* 2001 [8]	100	HA, 80 wt.%, 0.5–0.7 mm	176 °C, 98.1 MPa, 60 min	No			38	2000		
		nHA, 80 wt.%, 100 nm					72	3500		
	430	HA, 80 wt.%, 0.5–0.7 mm	184 °C, 98.1 MPa, 60 min	No			50	2500		
		nHA, 80 wt.%, 100 nm	194 °C, 98.1 MPa, 60 min	No			139	10,000		
Jing *et al* 2005 [5]	300	None	175 °C, 10 MPa, -	No	60	1800			n.a.	n.a.
				115 °C, 1 h	70	3100			120	3200
		Grafted nHA, 4 wt.%, 100×20–40 nm		No	63	2500			n.a.	n.a.
				115 °C, 1 h	74	3250			127	3750

DSC measurements show no evidence of polymer alteration nor crystallization degree according to the different treatments. The degree of crystallinity is most affected by the cooling rate during the process, which was slow enough. It would be interesting to check the effect of nHA content on the number and size of polymer crystallites.

The presence of HA nanoparticles obviously improves the mechanical strength and stiffness of the PLLA composites. Increasing the mineral content changes the fracture mode from plastic to brittle.

As said in introduction, it is difficult to compare results with those found in literature. Many factors influence the mechanical properties. Table 6 displays several examples of dense composites properties according to initial PLLA molecular weight, the nature of fillers, the process conditions and annealing treatment. Okuno et al. [17] have achieved superior properties without any filler by forging their samples. Here the introduction of micro-hydroxyapatite reduces tensile and compressive strengths but increases the different elastic moduli (tensile, compressive and bending). The effect of micro-fibers demonstrated by Abe et al. [9] is very high on bending modulus but has a negative effect on bending strength. In the case of addition of nanoparticles [5,8], better results are obtained in terms of mechanical strengths and moduli.

It appears that there is a strong interaction between process conditions and filler addition. The mixing technique, not clearly investigated in literature, is probably a key point. The optimum filler concentration can change from 4 wt.% to 80 wt.%. This final concentration of HA is also expected to affect the biological response.

5. Conclusion

This study shows that dense HA/PLLA composites with superior mechanical performances, close to those of cortical bone, can be prepared by dispersing HA nanoparticles into a PLLA matrix. Thus, commercial HA was thoroughly deagglomerated by wet attrition milling, and subsequently transferred by solvent exchange into a PLLA-chloroform solution. By this way, dense nHA/PLLA composites containing up to 46 wt.% uniformly dispersed HA nanoparticles were prepared. Microscopic observation has shown that HA particles remain uniformly dispersed at the nano-scale throughout the preparation steps. Mechanical tests have shown that, upon increasing the HA content, the strength and elastic modulus of the composite were significantly increased. At higher mineral contents, the rupture mechanism of the composite changes from ductile to brittle.

A further step towards the development of high performance bioresorbable bone substitutes would be to prepare these promising nHA/PLLA composites with adequate interconnected porous structure.

Acknowledgements

This work is part of the project NANOBIOCOM NMP3-CT-2005-516943, funded by the 6th Framework Programme of the European Community. This contribution is gratefully acknowledged by the authors. The authors would like also to thank the Interdisciplinary Centre for Electron Microscopy (CIME) at EPFL for its valuable assistance.

References

[1] J.M. Karp, P.D. Dalton, M.S. Shoichet, Mrs Bulletin 28 (2003) 301.
[2] D. Garlotta, Journal of Polymers and the Environment 9 (2001) 63.
[3] G. Perego, G.D. Cella, C. Bastioli, Journal of Applied Polymer Science 59 (1996) 37.
[4] J. Russias, E. Saiz, R.K. Nalla, K. Gryn, R.O. Ritchie, A.P. Tomsia, Materials Science & Engineering C-Biomimetic and Supramolecular Systems 26 (2006) 1289.
[5] Z.K. Hong, P.B. Zhang, C.L. He, X.Y. Qiu, A.X. Liu, L. Chen, X.S. Chen, X.B. Jing, Biomaterials 26 (2005) 6296.
[6] N. Pramanik, S. Mohapatra, P. Pramanik, P. Bhargava, Journal of the American Ceramic Society 90 (2007) 369.
[7] S. Sanchez-Salcedo, I. Izquierdo-Barba, D. Arcos, M. Vallet-Regi, Tissue Engineering 12 (2006) 279.
[8] N. Ignjatovic, K. Delijic, M. Vukcevic, D. Uskokovic, Bioceramics 192-1 (2000) 737.
[9] T. Kasuga, Y. Ota, M. Nogami, Y. Abe, Biomaterials 22 (2001) 19.
[10] N. Ignjatovic, E. Suijovrujic, J. Budinski-Simendic, I. Krakovsky, D. Uskokovic, Journal of Biomedical Materials Research Part B-Applied Biomaterials 71B (2004) 284.
[11] J.C. Middleton, A.J. Tipton, Biomaterials 21 (2000) 2335.
[12] W.J.E.M. Habraken, J.G.C. Wolke, J.A. Jansen, Advanced Drug Delivery Reviews 59 (2007) 234.
[13] R.Z. LeGeros, J.P. LeGeros, Bioceramics 15 (240-2) (2003) 3.
[14] E.R. Ruiz-Hitzky, M. Darder, P. Aranda, Journal of Materials Chemistry 15 (2005) 3650.
[15] V. Thomas, D.R. Dean, Y.K. Vohra, Current Nanoscience 2 (2006) 155.
[16] M. Darder, P. Aranda, E. Ruiz-Hitzky, Advanced Materials 19 (2007) 1309.
[17] Y. Shikinami, M. Okuno, Biomaterials 20 (1999) 859.
[18] A.G. Mikos, A.J. Thorsen, L.A. Czerwonka, Y. Bao, R. Langer, D.N. Winslow, J.P. Vacanti, Polymer 35 (1994) 1068.
[19] C. Schugens, V. Maquet, C. Grandfils, R. Jerome, P. Teyssie, Journal of Biomedical Materials Research 30 (1996) 449.
[20] G.B. Wei, P.X. Ma, Biomaterials 25 (2004) 4749.
[21] L.M. Mathieu, T.L. Mueller, P.E. Bourban, D.P. Pioletti, R. Muller, J.A.E. Manson, Biomaterials 27 (2006) 905.
[22] D.W. Hutmacher, Biomaterials 21 (2000) 2529.
[23] C. Pittet, J. Lemaitre, Journal of Biomedical Materials Research 53 (2000) 769.
[24] K.A. Ravaglioli, Bioceramics: Materials, Properties, Applications, London, Chapman & Hall, 1992, p. 44.